

# The Yuli Belt in Taiwan: Part of the suture zone separating Eurasian and Philippine Sea plates

Yiqiong Zhang, Chin-Ho Tsai, Nikolaus Froitzheim, and Kamil Ustaszewski

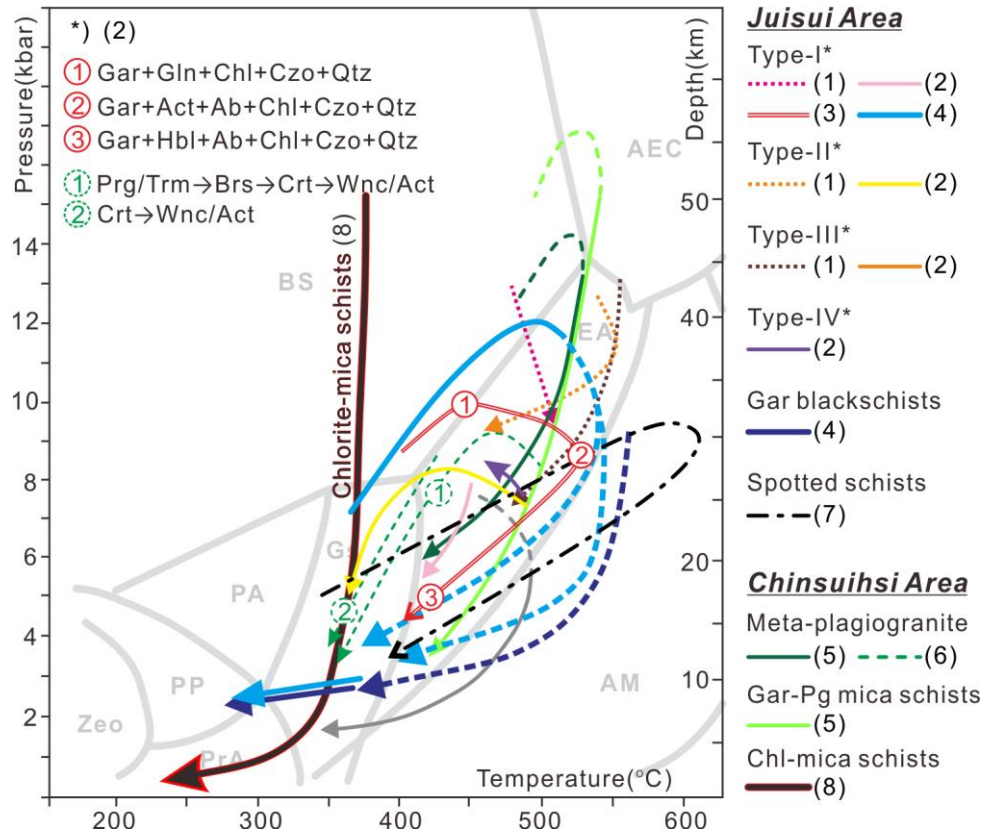


Fig. S1. P-T diagram (simplified after Maruyama et al. 1986) showing calculated metamorphic conditions and P-T-t paths suggested for high-pressure rocks in the Yuli belt with various metamorphic parageneses, as well as for a chlorite-mica schist from the metasedimentary unit (bold path-8). Type-I (Amp + Qz + Ep + Gar+ Chl + Rt/Ttn; Type-II: Pg + Amp + Qz + Ep + Gar + Chl + Ttn + Bt + Mag), Type-III (Amp + Qz + Ab + Ep + Gar + Rt + Hem + Ttn), and Type-IV (Amp +Ep + Pg+ Qz + Ab) are from Tsai et al. (2013). Mineral abbreviations follow those of Whitney and Evans (2010). Other abbreviations are Zeo, zeolite facies, PP, prehnite-pumpellyite facies; PA, pumpellyite–actinolite facies; PrA, prehnite-actinolite facies; GS, greenschist facies; EA, epidote-amphibolite facies; AM, amphibolite facies; BS, blueschist facies; AEC, amphibole eclogite facies. Sources: (1) Baziotis et al. 2017; (2) Tsai et al. 2013; (3) Sandmann et al. 2015; (4) Beyssac et al. 2008; (5) Lan et al. 1996; (6) Lo 2018; (7) Chiang 2003; (8) Conand et al. 2020.

# The Yuli Belt in Taiwan: Part of the suture zone separating Eurasian and Philippine Sea plates

Yiqiong Zhang, Chin-Ho Tsai, Nikolaus Froitzheim, and Kamil Ustaszewski

Table S1. Summary of deformation phases of the Yuli Belt metasediments from previous studies.

Reference	Area	Method	Deformation phases and age (if any)
Stanley et al. 1981	Southern Cross island highway	Schistosity and folding crosscutting relationships; Lithological correlations	<p><b>S1</b> = Cryptic  <b>S2</b> = Penetrative axial surface  <b>F2</b> = West vergent folds and faults  <b>S3</b> = NE strike; W dipping; Crenulation cleavage  <b>F3</b> = East verging; hinge plunge NE  <b>S4</b> = NE strike; NW dip; <b>F4</b> = minor folds deforming  <b>F5 and F6</b> = kink folds; variable orientation; flexing of dominant schistosity</p>
Pelletier and Hu 1984	Southern Cross Island Highway; East and South Taiwan	Structural analysis	<p><b>F0</b> = southward directed slumps  <b>D1</b> = EW to NW-SE compression; <b>S1</b> = Axial planar  <b>T1</b> = west vergent thrust  <b>F2</b> = kink-folds verging to the East, backfolding  <b>S2</b> = Crenulation cleavage  <b>F3</b> = North verging, E-W axis</p>
Hu and Tsan 1984	Southeastern Taiwan, Central Range	Structural and sedimentological analysis	<p><b>F0</b> = NS (EW depositional folds)  <b>S2</b> = NWW-SEE (NS-overtured tight folds and cleavage)  <b>D3</b> = bending of S2 cleavage</p>
Faure et al. 1991	Central and Southern cross island highway	Microstructural analysis and synthesis of previous works	<p><b>S1</b> = fracture cleavage (in the W. slate belt)  <b>F1</b> = overturned to the west (in slate belt)  <b>L1</b> = non-coaxial, top to the NW shear sense  <b>D2</b> = 3.5 Ma (Pelletier and Stephan 1986)  <b>F2</b> = overturned to the E., axis trend 100N (back folding);  <b>S2</b> = axial planar crenulation  <b>F3</b> = axis S dipping  <b>D4</b> = Normal faulting</p>
Clark et al. 1992	Northern and Southern Cross Island Highway	Microstructural analysis (syntectonic fibrous growth orientation)	<p><b>D1; D2; D3 = D2; D4</b> of Stanley et al. 1981  <b>S1</b> = dipping ~40SE; <b>L1</b> = updip; Clockwise rotation of elements + asymmetric folds and boudins → non-coaxial (simple shear)  <b>S2</b> = crenulation cleavage with fanning structure  <b>F2</b> = west vergent folds and axis dipping ~35° to the NE  <b>L2</b> = indicate fold-axis parallel extension and left-lateral shear  <b>Normal Faults</b> = <math>\sigma_3</math> plunge towards the NE, parallel to S2</p>

# The Yuli Belt in Taiwan: Part of the suture zone separating Eurasian and Philippine Sea plates

Yiqiong Zhang, Chin-Ho Tsai, Nikolaus Froitzheim, and Kamil Ustaszewski

Reference	Area	Method	Deformation phases and age (if any)
			<b>S3</b> = crenulation cleavage dipping NW, locally transposing <b>S2</b> (in the east)
Fisher 1999; Fisher et al. 2002	Easternmost Backbone Slates	Structural and microstructural analysis	<b>S2</b> = local crenulation, moderately W dipping <b>F2</b> = axis gentle NE plunging. <b>L2</b> = moderately NE dipping <b>Normal Faults</b> = late W-dipping
Yeh 2004	Eastern Central Range	Structural and microstructural analysis	<b>S0</b> = 37/096, overturned <b>S1</b> = 31/075 strong pervasive slaty cleavage <b>S2</b> = 36/308 pervasive foliation <b>F2</b> = kink-folds verging to the East; backfolding <b>S3</b> = 27/215, slaty cleavage <b>F3</b> = kink-folds verging to the North; fold axis 21/025 <b>S4</b> = weak crenulation cleavage <b>Normal Faults</b> = 45/045, 45/205, top-to-NE/SW shear
Ho and Lo 2015	Shoufeng Hsi (Wanjung area)	Structural and microstructural analysis	<b>S1</b> = commonly destroyed; in the microlithon <b>S2</b> = moderately NW dipping <b>F2</b> = east-vergence isoclinal folding <b>S3</b> = sub-horizontal axial plane cleavage <b>F3</b> = recumbent folds; fold hinge plunge NW
Ho 2015	Southern Cross Island Highway	Structural and microstructural analysis	<b>S1; S2; S3</b> of Ho and Lo 2015 <b>Normal Faults</b>
Mondro et al. 2017	Eastern Central Range (Eocene slates)	Syntectonic fibrous growth orientation	<b>S2</b> of Fisher et al. 2002 bulk coaxial strain and lateral extrusion effects